Bioelectromagnetics 26:275–286 (2005)

Time Dependent Modifications of Hep G2 Cells During Exposure to Static Magnetic Fields

Alfonsina Chionna, Bernadette Tenuzzo, Elisa Panzarini, Majdi B. Dwikat, Luigi Abbro, and Luciana Dini*

Department of Biological and Environmental Science and Technology, University of Lecce, Lecce, Italy

Morphological modifications, i.e., cell shape, cell surface sugar residues, cytoskeleton, and apoptosis of Hep G2 cells during 24 h exposure to 6 mT static magnetic field (static MF) were studied by means of light and electron microscopy and cytochemistry. Progressive modifications of cell shape and surface were observed during the entire period of exposure to static MF. Control cells were polyhedric with short microvilli covering the cell surface, while those exposed to static MF, were elongated with many irregular microvilli randomly distributed on the cell surface. At the end of the exposure period, the cells had a less flat shape due to partial detachment from the culture dishes. However, throughout the period of exposure under investigation, the morphology of the organelles remained unmodified and cell proliferation was only partially affected. In parallel with cell shape changes, the microfilaments and microtubules, as well as the quantity and distribution of surface ConA-FITC and *Ricinus communnis*-FITC labeling sites, were modified in a time dependent manner. Apoptosis, which was almost negligible at the beginning of experiment, increased to about 20% after 24 h of continuous exposure. The induction of apoptosis was likely due to the increment of $[Ca^{2+}]_i$ during exposure. In conclusion, the data reported in the present work indicates that 6 mT static MF exposure exerts time dependent biological effects on Hep G2 cells. Bioelectromagnetics 26:275–286, 2005.

Key words: cell shape; F actin; β-tubulin; sugar residues; apoptosis

INTRODUCTION

At the current state of knowledge, the biological effects, both in vivo and in vitro, of static or oscillatory electromagnetic fields (static MFs or ACEMFs) have yet to be unequivocally interpreted. The increasing production of EMFs due to the expanding use of electronic devices in normal life is favoring studies of these effects; the importance of fully understanding the true mode of action of (E)MFs on plant and animal cells arises from the need to better protect human health against their possible harmful effects [Kheifets, 2001; Wartenberg, 2001; Karasek and Lerchl, 2002].

The considerable interest in the influence of static MFs on biological systems has been a topic of research for many years [Rosen, 2003]. These fields are usefully classified as weak (<1 mT), moderate (1 mT–1 T), strong (1 T–5 T), and ultra-strong (>5 T). Weak geomagnetic fields are used by many organisms for spatial orientation and navigation. These organisms have developed systems that employ biogenic magnetite as field sensors [Hong, 1995]. The effects that have been attributed to strong and ultra-strong MFs are related to their tendency to alter the preferred orientation of a variety of diamagnetic anisotropic organic molecules. However, the effects of these fields also include alteration of the cleavage planes of *Xenopus* eggs, electroencephalograms of monkeys and visual behavior [Denegre et al., 1998; Rosen, 2003]. Conversely, although the effects of static MFs in the moderate range have been largely examined in several biosystems, the results obtained are often inconsistent.

It has been suggested that static MFs alter the function of the organism's transmembrane calcium flux in diverse experimental models [Rosen and Rosen, 1990; Fanelli et al., 1999; Teodori et al., 2002a]. A general mechanism for the action of moderate intensity static MFs on biological systems would be by virtue of their effect on the molecular structure of excitable membranes, an effect sufficient to modify the function of embedded, ion specific channels. This hypothesis

*Correspondence to: Prof. Luciana Dini, Department of Biological and Environmental Science and Technology, University of Lecce, via per Monteroni, 73100 Lecce, Italy MIUR Grant.
E-mail: luciana.dini@unile.it

Received for review 29 January 2004; Final revision received 20 June 2004

DOI 10.1002/bem.20081
Published online in Wiley InterScience (www.interscience.wiley.com).

would explain virtually all of the bioeffects attributed to these fields and is testable using several different neurophysiological techniques [Rosen, 2003].

Living cells and organisms are able to respond to a wide range of environmental stimuli and stressors, including electric or magnetic fields [(E)MFs], leading to intracellular and extracellular changes [Saffer and Phillips, 1996], which can be classified as irreversible/reversible or structural/functional, and changes to cells and their organelles. The cellular and molecular modifications induced when (E)MFs interact with biological materials are, however, dependent on the duration of exposure, tissue penetration, and heat generation, which in turn are related to their intensity and frequency. In addition, cellular responses depend not only on the intensity and frequency of the field, but also on the type of field (static or oscillatory), of the waveform (sinusoidal, square, etc.) and on the biological status of the exposed cells [Cossarizza et al., 1989; Walleczek and Liburdy, 1990]. Most of the theories addressing the mechanism of interaction between biological systems and (E)MFs suggest that the plasma membrane, by virtue of its bioelectrical properties, is the site where (E)MFs exert their primary effects [Repacholi, 1998; Teodori et al., 2002b; Rosen, 2003]. Structural and biophysical changes to the plasma membrane are likely to affect, in turn, receptor binding and activation, and thereby cell function in general. The described membrane responses to MFs are consistent with the demonstrated reorientation of diamagnetic molecular domains within the membrane [Rosen, 1993].

It is generally known that morphological and structural changes to the plasma membrane interfere with many functional and structural features of the cells, leading, for example, to changes in cellular shape, cytoskeleton arrangement, ions flux, receptor distribution, phagocytosis, etc. In the present study, we report that 6 mT static MF affects the shape of Hep G2 cells, the integrity of the plasma membrane and cytoskeleton and influence the rate of apoptosis.

MATERIALS AND METHODS

Cell Culture: Hep G2 Cells

The Hep G2 cells, a hepatic transformed cell line and the cellular system the authors are best acquainted with, were cultured in DMEM medium (Cambrex, Verviers, Belgium) supplemented with 10% fetal bovine serum, L-glutamine (2 mM) (Cambrex), penicillin and streptomycin solution (100 IU/ml), and nystatin (antimycotic solution) (Sigma, St. Louis, MO) (10000 U/ml or 0.05 mg/ml) (Cambrex). The cells were incubated at 37 °C in a humidified atmosphere of 5% CO_2. Stock cultures of Hep G2 cells were maintained in 75 cm^2 flasks and the culture medium was changed every 2 days. Cells grew continuously and doubled approximately every 2 days. When the cells reached confluence they were detached from the flask with 0.25% trypsin plus 0.02% EDTA (Cambrex) in normal saline for 5–7 min at 37 °C and then diluted with fresh medium and centrifuged at 800 rpm for 10 min. The cells were seeded at a density of 1.5×10^5 cells per well in 24 well plates containing the prepared circular cover slip for SEM preparation, and at a density of 15×10^5 cells in each 75 cm^2 flask for TEM examination. For the static MF exposure experiments, cells were cultured in Petri dishes (3.2 cm dia) at a concentration of 5×10^4 cells/ml. Cells were allowed to attach for 24 h and then exposed to static MF. The concentration of cells was determined by a Bürker's chamber.

Cell Growth Rate

Cells were cultured in 24 well dishes in the presence or the absence of the static MF. The growth rate of the cells was assayed using a Cell Counting kit-1 (Dojindo Laboratories, Tokyo, Japan), based on the conversion of 2-(4-iodophenyl)-3-(4-nitrophenyl)-5-(2,4-disulfophenyl)-^{2}H-tetrazolium monosodium salt (WST-1) into WST-1 formazan by succinate-tetrazolium reductase. This enzyme is a part of the mitochondrial respiratory chain and is active in viable cells. All manipulations were performed according to the manufacturer's instructions. Reaction was stopped by the addition of 10 µl of 0.1 N HCl to each incubation well. Measurements were taken using a Jasco FP-750 spectrofluorometer at 450 nm.

Magnetic Field Application

Static MF was produced by Neodymium magnetic disks, 10 mm in diameter and 5 mm in height, of known intensity supplied by Calamit Ltd. (Milano, Italy) placed under the culture Petri dishes. The intensity of the field generated by the magnet was checked by means of a gaussmeter (Hall effect gaussmeter, GM04 Hirst Magnetic Instruments Ltd., UK). Since Hep G2 cells are monolayer-growing cells, field intensity of 6 mT is obtained on the bottom of the culture dish at 2.5 cm from the magnet. This distance was obtained by interposing between the magnetic disk and the Petri dish two disks of the same diameter as the culture dish, one metallic disk (in order to minimize the differences in the field intensity across the whole bottom of the dish) and one of inert material. Figure 1 reports the field intensities measured in three different zones of the dish bottom. Static MF was applied continuously for up to 24 h, unless otherwise specified. During the 24 h of experiment no increase in temperature was observed.

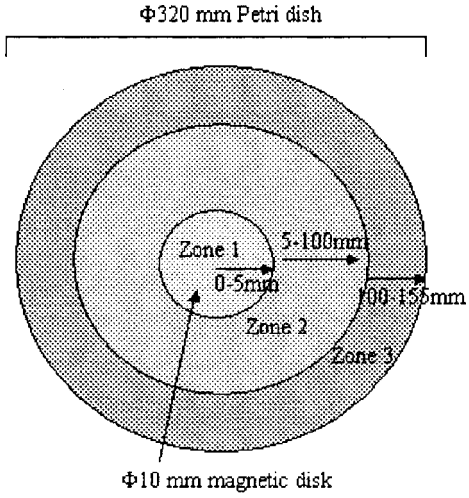

Fig. 1. Schematic view from above, showing the magnetic field distribution in three different zones of the bottom of the Petri dish. Zone 1 corresponds to the area of the magnetic disk, with field intensity of 6.00 ± 0.01 mT. In zone 2, corresponding to the area from 5 to 100 mm from the centre of the dish, an intensity of 5.90 ± 0.06 mT was measured. Zone 3 corresponds to the peripheral part of the culture dish (area 100–155 mm from the centre of the dish) in which a field intensity of 5.9 ± 0.1 mT was measured.

Dishes of cells were always placed on the same two shelves in a tissue culture incubator where the ambient 50 Hz magnetic field was 0.95/0.62 μT (heater on/off) and static magnetic flux density was 5.5 μT. In the laboratory areas where the cells were processed (between incubators and worktops) the field measured ranged between 0.08 and 0.14 μT (50 Hz) magnetic fields.

Exposures were carried out in a blind manner. Simultaneously experiments, omitting the magnets were, performed as controls. Cells were monitored at fixed interval times up to 24 h (1, 2, 4, 8, 18, 24 h).

Quantification of Apoptosis and Proliferation

The evaluation of the percentage of apoptotic and viable cell fractions was performed with different techniques: light microscopy of hematoxylin/eosin stained cells, Hoechst-33342 labeled cells, DNA laddering, and flow cytometry. Cell viability was also assessed by membrane impermeability to trypan blue. Cell growth was evaluated by counting the cells during 5 days of culture in the presence and absence of 6 mT static MF.

Light microscopic analysis of apoptosis, done on Hoechst-33342 or hematoxylin/eosin stained cells, also made it possible to measure the presence of necrotic cells. The fraction of cells with fragmented, crescent-shaped or shrunken nuclei (all apoptotic morphologies) were evaluated by counting at least 500 cells in at least ten randomly selected fields.

Flow cytometry was performed with an EPICS XL flow cytometer (Coulter Electronic, Inc., Hialegh, FL) equipped with a 5 W argon laser having a 488 nm excitation wavelength. The fixed cells were stained with propidium iodide (10 μg/ml) in phosphate buffered saline containing 40 U/ml RNAse and 0.5% Tween-20. The 635 nm emission wavelength was monitored for propidium iodide emission. By considering the flow cytometry of propidium iodide stained cells it was possible to analyze the percentage of diploid, hypodiploid, and tretraploid cells according to the amount of DNA per event detected by the flow cytometer. Apoptotic cells are characterized by a low amount of DNA and their percentage can be determined from the cytograms. The stage of the cell cycle is determined by the amount of propidium iodide incorporated. Histograms of relative DNA content were analyzed by using Multicycle software to quantify the percentage of cells at each stage of the cell cycle. Data are reported here as the fraction of apoptotic, (sub-G_1 peak), proliferating (S peak), and viable (G_1/G_0 peak) cells. For each of the flow cytometry analyses at least 10000 events were calculated.

Apoptosis is also characterized by DNA fragmentation. A total of 10^6 cells were lysed in a buffer containing 10 mM EDTA, 100 mM Tris (pH 8), 0.5% sodium lauroyl sarkosine and 200 μg/ml proteinase K. Nucleic acids were extracted with phenol (chloroform:isoamylic alcohol 24:1) and ethanol, and then precipitated and incubated in 100 μg/ml RNase A for 60 min at 37 °C. The purified DNA was loaded on a 1.5% agarose gel in TAE buffer, stained with 10 μg/ml ethydium bromide, and visualized on a 254 nm UV transilluminator.

The scoring of cells in mitosis and the scoring of the morphologies (normal or altered) was evaluated on hematoxylin–eosin sections. The number of mitotic and apoptotic cells and the number of cells with normal or altered morphologies was randomly measured in 50–100 high power microscopic fields (60×). Approximately 5000 nuclei per sample were counted. The values were expressed as the number per microscopic field.

Ca^{2+} Levels

Cells (5×10^7 cells at a concentration of 1×10^6/ml) were washed twice with loading buffer (120 mM NaCl, 5.4 mM KCl, 4.2 mM $NaHCO_3$, 1.2 mM KH2PO_4, 1.3 mM $CaCl_2$, 1.3 mM $MgSO_4$, 20 mM HEPES, 15 mM glucose, 2% BSA equilibrated with CO_2), resuspended at a final concentration of 2×10^7 cells/ml and then loaded with 4 μM fura-2 acetoxymethylesther (FURA 2-AM) (Sigma) for 30 min at room temperature. After the dye loading procedure,

cells were washed twice with the same loading buffer and then resuspended in fresh loading buffer at the final concentration of 3×10^6 cells/ml. Cells were stored at room temperature until use and prewarmed at 37 °C for 2 min before measurements. The fluorescence of fura-2 was measured using a Jasco FP-750 spectrofluorometer, equipped with an electronic stirring system and a thermostabilized (37 °C) cuvette holder, and monitored by a personal computer running the Jasco Spectra Manager software for Windows 95 (Jasco Europe s.r.l., Lecco, Italy). The excitation wavelengths are 340 and 380 nm and the emission wavelength is 510 nm; the slit widths were set to 10 nm. Two milliliters of cell suspension at the final concentration of 3×10^6 cells/ml, was placed in a glass cuvette, and fluorescence values were converted to $[Ca^{2+}]_i$ values according to Grynkiewicz et al. [1995].

Transmission and Scanning Electron Microscopy

The ultrastructure of the Hep G2 cells was obtained with transmission (TEM) and scanning electron microscopy (SEM). At each experimental time, cells, seeded as reported above, were fixed with 2.5% glutaraldehyde in cacodylate buffer, pH 7.4, for 1 h at ice temperature and postfixed with 1% OsO_4 in the same buffer; afterwards samples were dehydrated, embedded in Spurr resin and examined under a Zeiss 910 transmission electron microscope operating at 80 kV. SEM observations were accomplished on cells seeded on circular coverslip slides. A Balzer 020 Critical Point Dryer and a Balzer 040 Sputter Coater were used for the final SEM preparation steps. Cells were examined under a Philips XL50 scanning microscope operating at 20 kV.

Lectins and Cytoskeleton Cytochemistry

Hep G2 cells, grown on circular coverslip slides, were fixed with 4% formaldehyde in phosphate buffer (pH 7.4) for 10 min and analyzed for surface localization of sugars by using Concanavalin-A (Con-A) (40 μg/ml mannose) and *Ricinus communnis* (2 μg/ml D-galactose) FITC conjugates for 30 min in the dark. For cytoskeletal proteins, either a rabbit anti-β-tubulin (diluted 1:10 in 3% BSA in PBS and revealed by a Texas red-conjugated anti-rabbit-IgG antibody) for 1 h or a 10 μM FITC-conjugated phalloidin for 20 min were used. All the incubations were performed at room temperature. After incubation the slides were finally washed with PBS and mounted in Mowiol. Samples were observed with a Nikon PCM 2000 microscope (Nikon, Tokyo, Japan) with Plan Fluor objectives (Nikon). Confocal microscopy was performed utilizing a Nikon PCM 2000 confocal laser scanning head based on a Nikon Eclipse 600 microscope, equipped with an Argon Laser ED HeNe 488 nm 543 source. Blind acquisition and visualization were completely computer controlled by the EZ 2000 software (Coord-Nikon, the Netherlands). Lectins, anti-β-tubulin and phalloidin-FITC were all purchased by Sigma.

Statistical Analysis

Statistical analyses were performed using one-way analysis of variance (ANOVA) with 95% confidence limits. Data are presented in text and figures as mean ± SD.

RESULTS

Viability, Apoptosis, Proliferation, and $[Ca^{2+}]_i$ Concentrations

Hep G2 cells were continuously exposed to 6 mT static MF for up to 24 h; and viability, apoptosis, and proliferation were monitored at fixed interval times (1, 2, 4, 8, 18, 24 h) by the trypan blue exclusion test (Fig. 2, panel A), hematoxylin/eosin staining (Fig. 2, panel B), flow cytometry analysis (Fig. 3, panels A,C), Hoechst 33342 labeling (Fig. 3, panel B), and DNA laddering (Fig. 3, panel D). The viability of Hep G2 cells not exposed to static MF did not change during the 24 h of monitoring; in all cases it was higher than 95% (Fig. 2, panels A,B). The viability of Hep G2 cells significantly decreased by about 20% during 24 h of continuous exposure (Figs. 2 and 3, panels A,C). The drop in viability was probably due to apoptosis (Fig. 2, panel B, and Fig. 3, panels A,C), which was more rapid than controls early during exposure and reached its maximum value at 24 h. Apoptosis above control values was observed in Hep G2 cells after 24 h of exposure to 6 mT static MF by using several techniques: flow cytometry (sub-G_1) (Fig. 3, panels A,C) showed alterations to the cell cycle; gel electrophoresis showed fragmented DNA (Fig. 2, panel D); light microscopy and transmission electron microscopy showed cells with condensed chromatin (Fig. 4, light microscopy and Fig. 5, electron microscopy). All this data support the pro-apoptotic effects of 6 mT static MF on Hep G2 cells.

The growth rate of Hep G2 cells was assayed for 5 days in the presence and absence of static MF. The number of viable cells at 24 h after cultivation was taken as a relative absorbance unit of WST-1 formazan and was plotted for all the other times (Fig. 4, panel B). As expected, Hep G2 control cells exhibited continuous growth in a monolayer and showed an epithelial morphology, doubling their number every 2 days (Fig. 4, panel B). In contrast, static MF exposure decreased the rate of growth after two days of

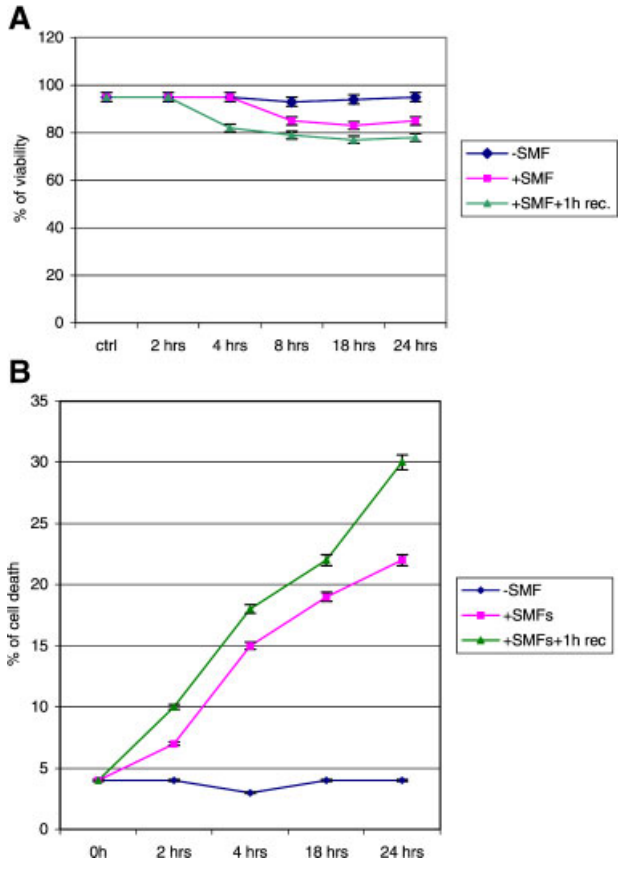

Fig. 2. Time course of viability (**A**) and cell death (**B**) in Hep G2 cell cultures in the absence or presence of 6 mT static MFs for up to 24 h or recovered 1 h after 24 h exposure. A: Trypan blue exclusion tests (percentage ± SD of viable cells), from counting at least 300 cells for each time point in at least ten randomly selected fields. B: Percentage apoptotic population counted as above on hematoxylin/eosin staining slides. [The color figure for this article is available online at www.interscience.wiley.com.]

continuous exposure. Indeed, when the proliferation was monitored during 24 h of exposure, the proliferation rate was about 10% greater than that of controls at both 18 and 24 h of treatment (Fig. 3, panels A–C).

Mitotic figures were observed frequently in these samples (Fig. 3, panel B). The modifications (apoptosis and cell shape) induced by static MF exposure lasted at least 1 h after the removal of the static MF and, in the case of apoptosis, were even higher than those measured during the exposure period.

$[Ca^{2+}]_i$ concentrations were measured with a spectrophotometer at fixed times during the exposure and after 1 h of recovery from exposure. $[Ca^{2+}]_i$ changed during the period under investigation; in particular, after 4 h of exposure the $[Ca^{2+}]_i$ concentration had increased by about 40%. A slow return to the normal values was observed afterwards (Fig. 5).

Cell Shape Modifications

Non-exposed Hep G2 control cells had a flat and polyhedric shape, tightly attached to the culture plate (Figs. 4 and 6); tiny short microvilli were randomly distributed on the cell surface. The thicker part of the cells contained the nucleus, while the cytoplasm expressed a large rough endoplasmic reticulum (RER), mitochondria and different sized vacuoles. Cell shape was extensively modified during 24 h exposure to 6 mT static MF (Fig. 4, panel A). Morphological modifications were directly analyzed by phase contrast microscope observation of living cells and by light and electron Microscope observation of fixed cells. Figures 3 and 6 summarize cell shape modifications of Hep G2 cells, progressively occurring over up to 24 h exposure to 6 mT static MF.

By comparing LM, SEM, and TEM micrographs the dramatic changes in cell shape were clearly seen. In particular, the exposed cells lost their polyhedric shape and acquired a fibroblast-like shape. The cytoplasm concentrated around the nucleus, making this part of the cells thicker and rounder. In synchrony with the shape modifications, the cell surface was covered with many round and/or lamellar microvilli, giving rise to rough, foamy-like surfaces (see SEM micrographs of Fig. 6 from 18 to 24 h under exposure to static MF). However, during the entire period of static MF exposure under investigation, even when cells became round and expressed many lamellar microvilli, neither cytoplasmic organelles or nuclei were modified, except in the apoptotic cells (see TEM micrographs of Fig. 6 from 18 to 24 h under exposure to static MF; last picture of second row is an apoptotic cell).

Cytoskeletal Modifications

The morphological changes above described were paralleled by the rearrangement of the cytoskeletal components: F-actin and β-tubulin reorganization was observed in cells exposed to static MF. In parallel with the cell shape changes, actin microfilaments, which were regularly distributed in the whole cytoplasm of control cells, became progressively organized into peripheral bundles, concentrated in the microvilli over time in exposed cells (Fig. 7). Tubulin microtubules formed a homogenous network around the nucleus of control cells, which became less organized over time in exposed cells (Fig. 7).

Cell Surface Sugar Residues

Modifications of cell surface expression of glycans (D-mannose and D-galactose residues), detected by ConA and *R. communis*-FITC conjugates, were studied by confocal microscopy in control and static

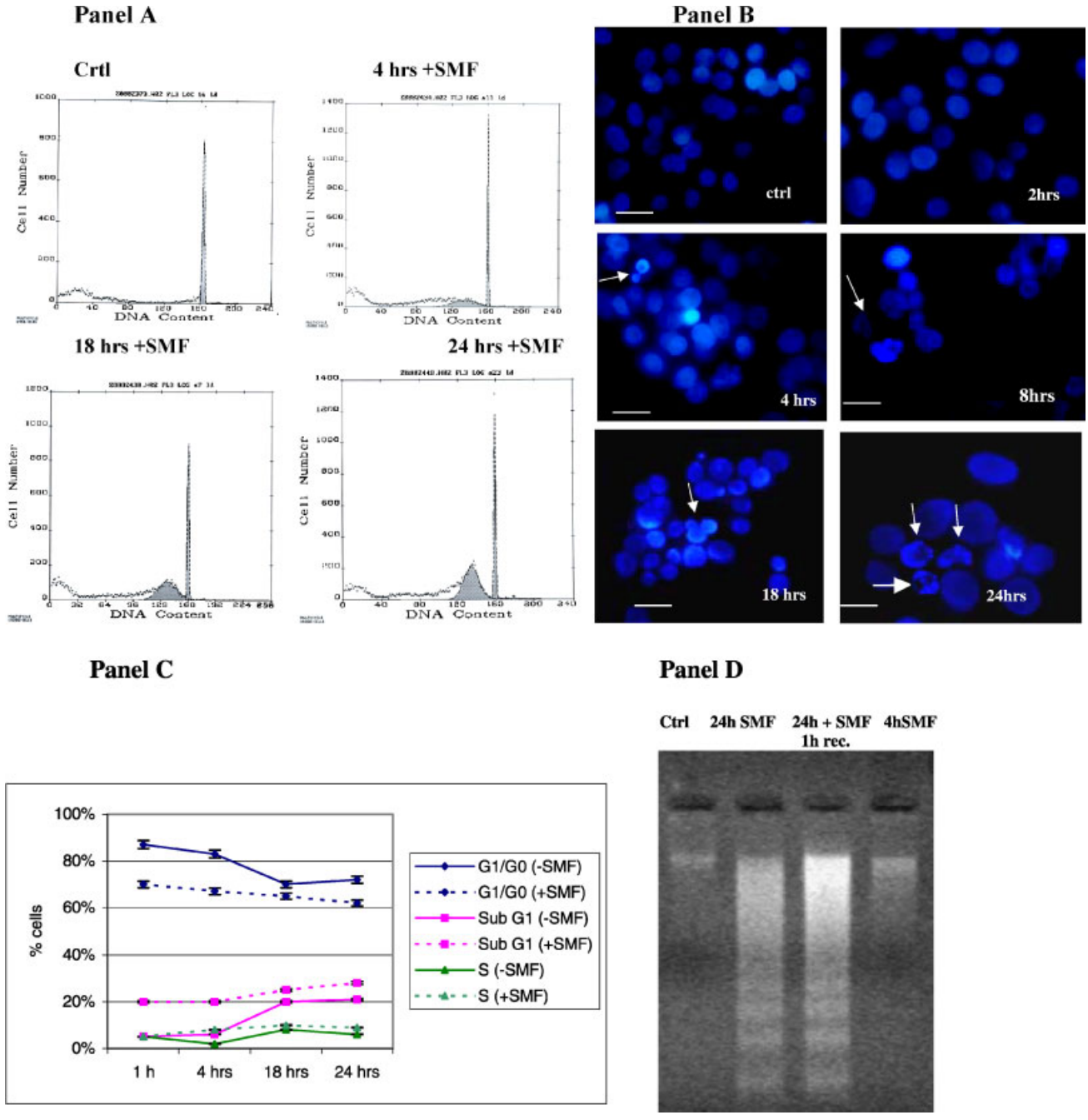

Fig. 3. **Panel A**: Effects of static MFs on cell cycle distribution and apoptosis induction in Hep G2 cells during 24 h exposure to 6 mT flux intensity. For each measurement at least 10 000 cells were counted. Representative results from three independent experiments are shown. **Panel B**: Static MFs increased the extent of apoptosis: morphological analysis. Representative time course photographs of Hoechst 33342-stained nuclei of Hep G2 cells during 24 h exposure to 6 mT static MFs. Small arrows indicate apoptosis. Large arrows indicate mitosis. Bars = 20 μm. **Panel C**: Percentage of Hep G2 cells in cell cycle phases in the presence and in the absence of 6 mT static MFs. The average values of three independent experiments, each performed in duplicate are reported. For each measurement at least 10000 cells were counted. **Panel D**: DNA from Hep G2 cells in the absence and in the presence of 6 mT static MFs on 1.5% agarose gel, as described in Materials and Methods. The ladder-like pattern of apoptosis is well evident in 24 h-exposed cells and cells after 1hr recovery after 24 h exposure. [The color figure for this article is available online at www.interscience.wiley.com.]

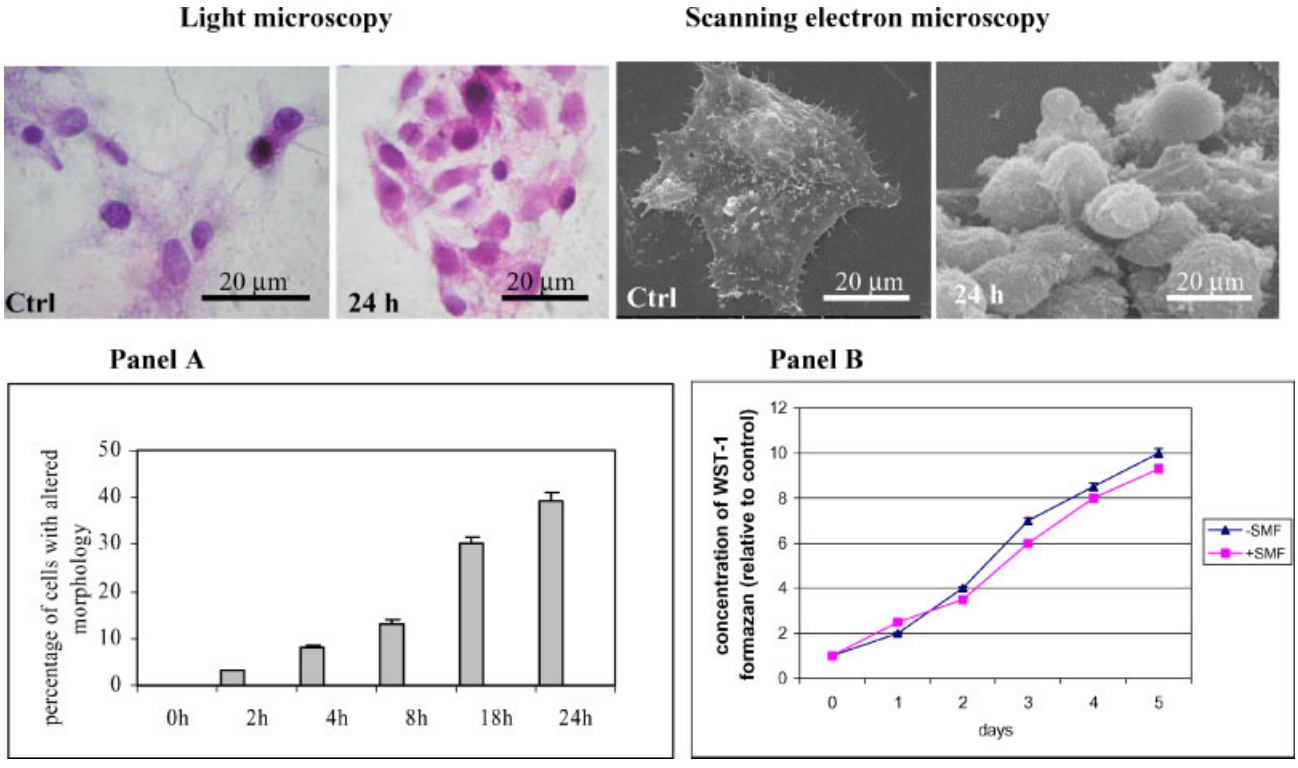

Fig. 4. Morphological modifications of Hep G2 cells exposed to static MFs of 6 mT for up to 24 h. **Panel A** indicates the percentage of cells with altered morphology (i.e., rounder and more fibroblast-like shape; see light and electron microscopy pictures). **Panel B** shows the growth rate up to 5 days of Hep G2 cells cultured in the presence or in the absence of 6 mT static MFs. Differences in cell shape between controls and 24 h-exposed cells is shown in the Light and SEM microscopy images. In particular, after 24 h of exposure cells have completely lost their typical flat and polyhedric shape. [The color figure for this article is available online at www.interscience.wiley.com.]

MF-exposed Hep G2 cells. D-galactose residues were mildly expressed on the surface of control cells (Fig. 8a), the intensity of fluorescence began to increase after 2 h and continued to increase for up to 24 h of exposure (Fig. 8b,c). The fluorescent labeling, randomly distributed all over the cell surfaces at short times of exposure, became concentrated in very bright fluorescent spots, mainly near the nucleus, at long times of exposure.

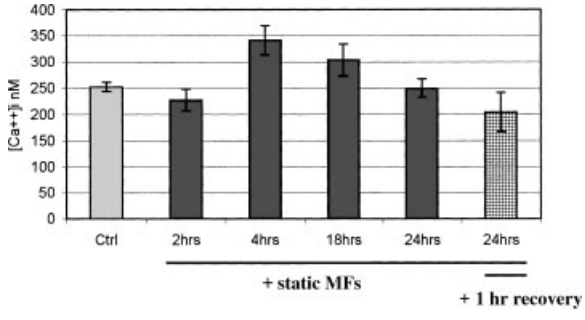

Fig. 5. Evaluation of the concentration of $[Ca^{2+}]_i$ by fura-2 in Hep G2 cells in the presence or absence of static. The data are the average ± SD of three independent experiments.

ConA binding sites, which were negligible in non-exposed control cells (Fig. 8A), progressively increased and, at 8 h of exposure (Fig. 8B) became concentrated into fluorescent bright spots all over the exposed Hep G2 cells. The fluorescent bright spots showed an further increased intensity and their size enlarged at the end of exposure time (Fig 8C).

DISCUSSION

In this study, we showed that 6 mT static MF exert a strong and replicable effect on cell shape and plasma membranes of Hep G2 cells. The research, which focused on cell shape and cell surface modifications, provided evidence for time related changes in shape, microvilli (number and shape), surface sugar residues and cytoskeleton organization. Modifications of cell shape and plasma membranes as a consequence of exposure to MFs or EMFs in other cell lines have also been reported recently [Hamada et al., 1989; Paradisi et al., 1993; Santoro et al., 1997; Lisi et al., 2000; Chionna et al., 2003; Rieti et al., 2004]. This indicates that morphological modifications may be considered a

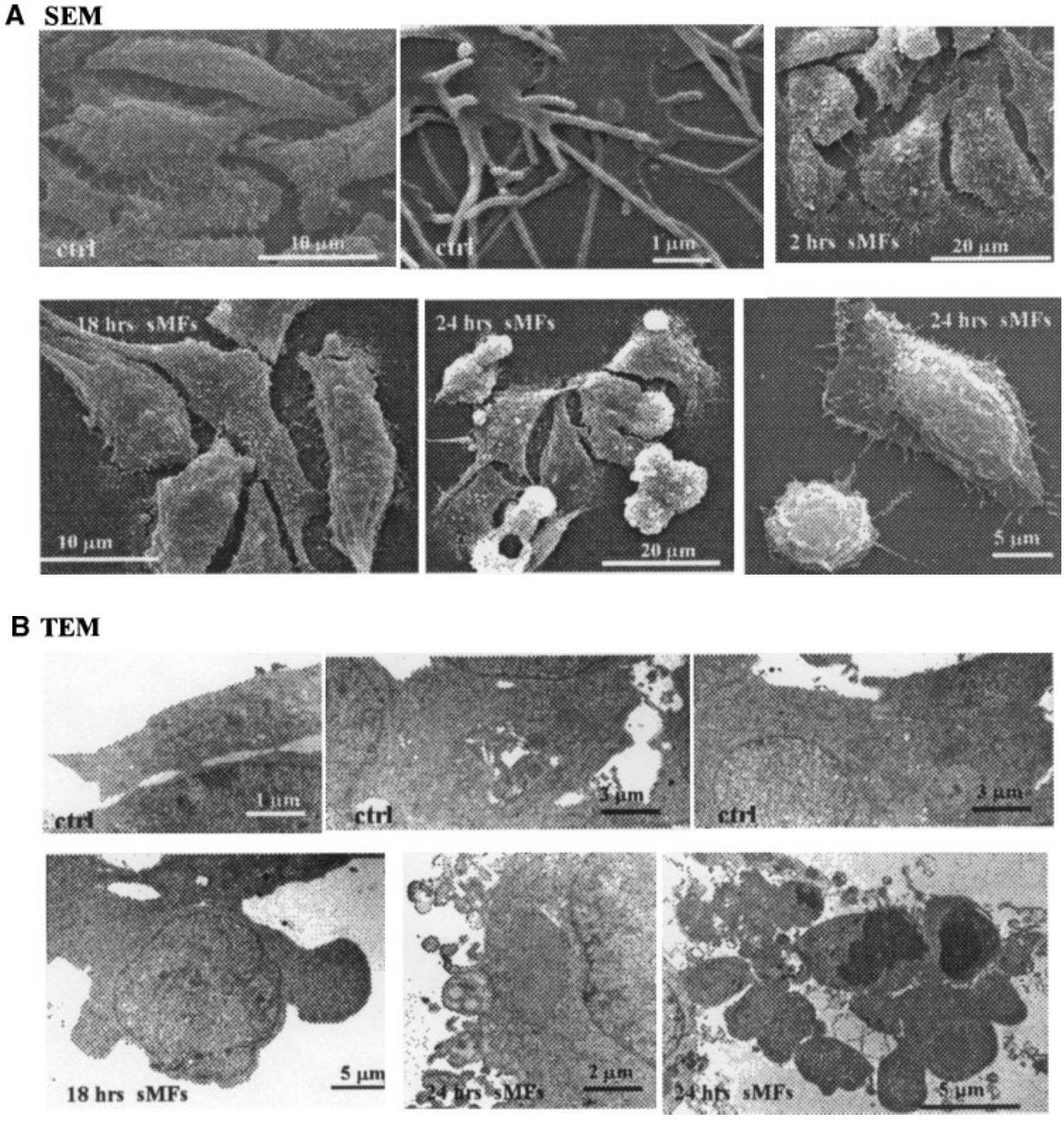

Fig. 6. **A**: SEM and (**B**) TEM micrographs showing the time course of cell shape modifications of Hep G2 cells exposed to 6 mT static MFs for 24 h. Non-exposed Hep G2 control cells are characterized by a flat and polyhedric shape with microvilli randomly distributed all over the cell surface or attached to the culture plate. The continuous exposure to static MFs for up to 24 h progressively modified cell shape, leading to the formation of lamellar and/or bubble-like microvilli or to induction of apoptosis. Mitochondria were well preserved even after 24 h of exposure to static MFs.

common stress response to exposure to static MFs, irrespective of cell type and species. Indeed, cell and surface modifications in response to exposure seems to be a highly conserved process, having been detected in invertebrate organisms as well [Ottaviani et al., 2002; Gobba et al., 2003]. However, we demonstrated that the extent of the modifications, within certain limits, is also determined by the time of exposure [Rosen, 1993; Chionna et al., 2003].

Control cells were tightly attached to the culture plate, but cells exposed to 6 mT static MF progressively shifted from a flat polyhedric shape towards a round or

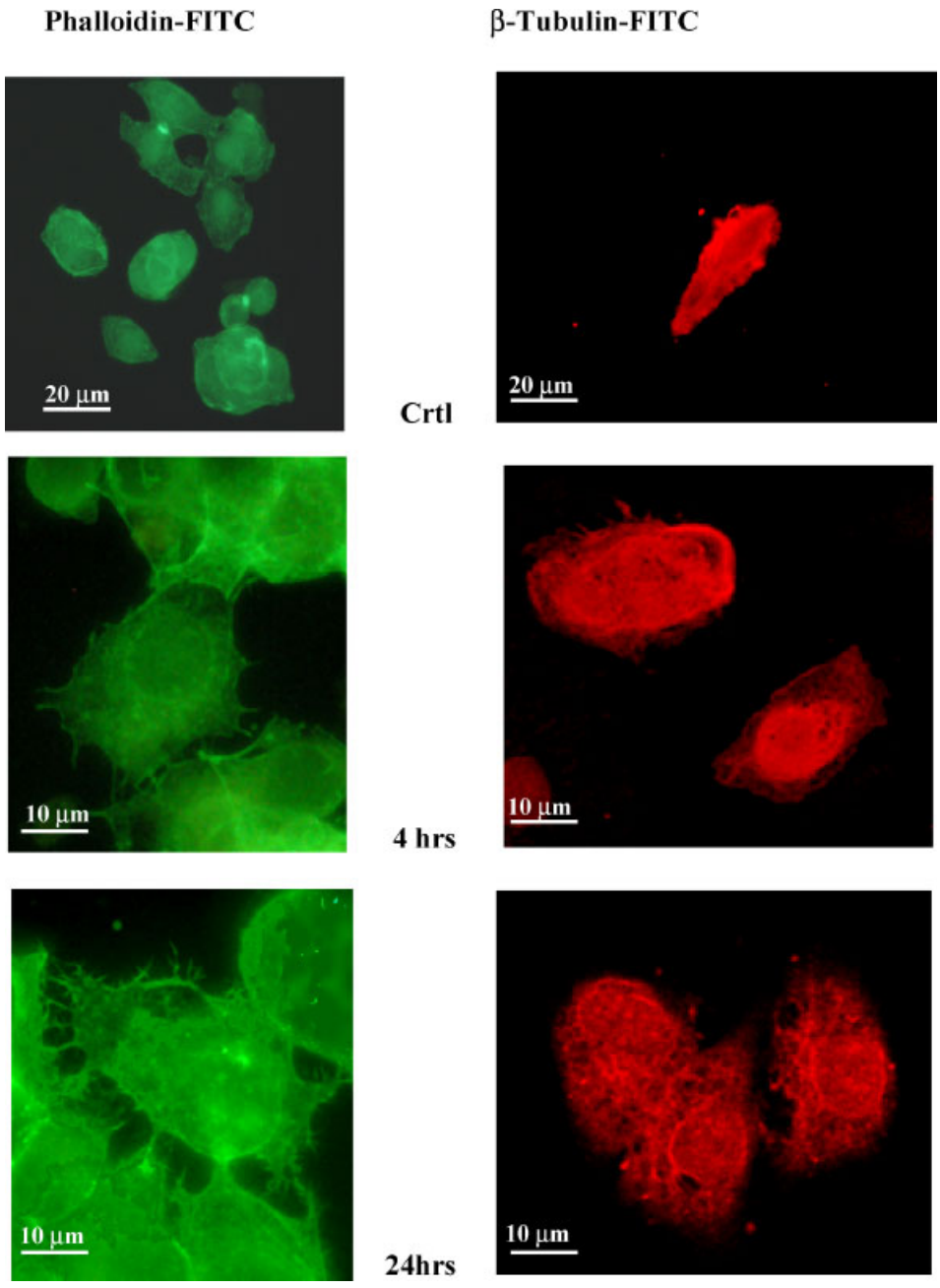

Fig. 7. Fluorescent micrographs of phalloidin-FITC and β-tubulin-TRICT labeling of Hep G2 cells. Phalloidin-FITC: random distribution of fluorescence in the whole cytoplasm of control cells. With increasing time of exposure to static MFs (from 4 to 24 h), actin microfilaments changed their organization and, at the longest time of exposure, concentrated in the microvilli as indicated by the high intensity of fluorescence. β-Tubulin-TRICT: tubulin microtubules formed a homogenous network around the nucleus, which became less organized with time of exposure. Bars = 10 and 20 μm. [The color figure for this article is available online at www.interscience.wiley.com.]

fibroblast-like shape. The presence of many lamellar or bubble-like microvilli has been already observed in previous reports using other cell types and other field types and intensities [Popov et al., 1991; Paradisi et al., 1993; Chionna et al., 2003]. The reason for such peculiar modification is still obscure; however, the appearance of lamellar or bubble-like microvilli can be viewed as an index of exposure. The actin base of the microfilaments that make up the microvilli has been recently argued to represent a cellular interaction site for magnetic fields [Gartzke and Lange, 2002]. Therefore, the general notion that magnetic fields regulate

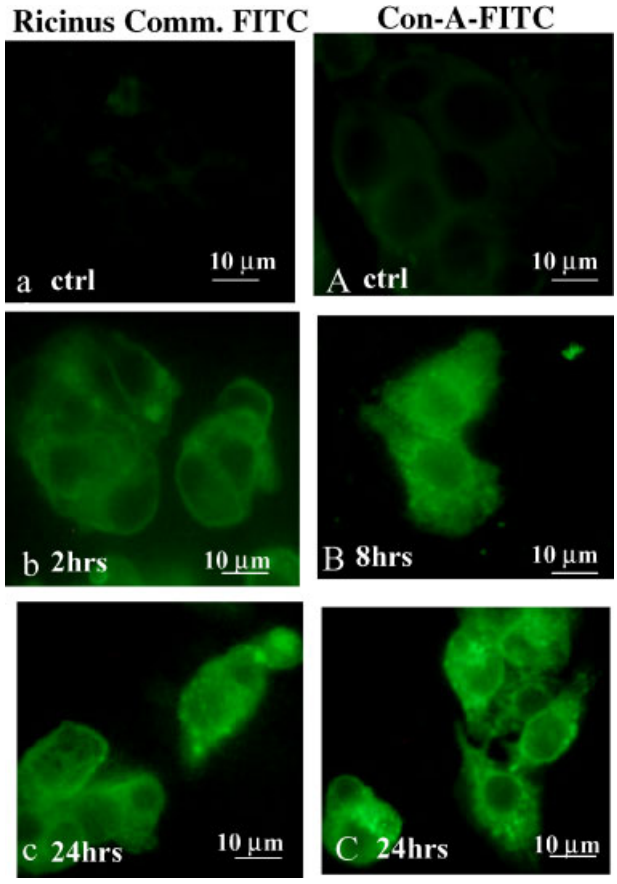

Fig. 8. Confocal micrographs of *Ricinus communis* (**a**–**c**) and ConA (**A**–**C**) binding sites on Hep G2 cells. Lectin FITC conjugates were used. D-galactose residues, not expressed on the surface of control cells increased progressively from 2 h of exposure to reach their maximum intensity at 24 h of exposure. The fluorescent labeling was randomly distributed on the cell surface at the short times of exposure, while at long times of exposure, fluorescence concentrated near the nucleus in very bright fluorescent spots. ConA binding sites were not expressed on the surfaces of control Hep G2 cells (A). The intensity of fluorescence began to increase from 2 to 24 h of exposure (b, c). The fluorescent labeling, randomly distributed all over the cell surfaces at short times of exposure, was concentrated in very bright fluorescent spots, mainly near the nucleus, at long times of exposure. Bars = 10 μm. [The color figure for this article is available online at www.interscience.wiley.com.]

ions and microvilli substrates, which provides a possible theoretical basis for understanding the physiological effects of even extremely low magnetic fields, could help to explain the formation of abnormally shaped microvilli.

Since $[Ca^{2+}]_i$ flux in Hep G2 was modified under static MF exposure, in agreement with other reports [Fanelli et al., 1999; Teodori et al., 2002a,b; Chionna et al., 2003], it could be hypothesized that lamellar or bubble-like microvilli represent the morphological evidence of the end point alteration of cellular functions to which Ca^{2+} ions contribute. The increase and mobilization of Ca^{2+} ions during static MFs exposure seems to be a crucial event in the cell: (a) some of the available studies suggest that the mechanism of reorganization and breakdown of different cytoskeleton elements is related to modified $[Ca^{2+}]_i$ homeostasis or the altered phosphorylation /dephosphorylation state of proteins in exposed cells [Popov et al., 1991; Santoro et al., 1997]; (b) decreased phagocytic uptake of latex microspheres is caused by increased intracellular $[Ca^{2+}]_i$ levels in macrophages [Flipo et al., 1998]; (c) the apoptotic rate falls with higher $[Ca^{2+}]_i$ levels [Fanelli et al., 1999; Teodori et al., 2002a,b; Chionna et al., 2003]. The influence of static MFs on $[Ca^{2+}]_i$ has been also reported in *Fusarium culmorum* giving rise to the modification of Ca^{2+} dependent signal transduction pathways involved in conidia germination [Albertini et al., 2003].

The increase and mobilization of $[Ca^{2+}]_i$ during exposure of Hep G2 cells to static MF can cause, directly or indirectly, a cascade of microfilament and microtubular reorganization, cell shape modifications, surface sugar residues, induction of apoptosis, etc. In particular, changes in cell shape and cell surface micromorphology in the exposed cells are more closely related to the reorganization of the cytoskeleton elements than to disruption, in agreement with the report of Bras et al. [1998], which suggests that cytoskeleton reorganization is due to promotion of assembly of their elements and to modulation of their orientation by high MFs in vitro. Indeed, cytoskeleton reorganization may modify cell surface sugar residues, whose amount and distribution was dependent on exposure time and sugar type. It is worth noting that modification of the expression and distribution of cell surface sugar residues is a marker of both aged and apoptotic cells [Dini, 2000; Savill and Fadok, 2000; Fadok and Chimini, 2001; Dini et al., 2002]. In particular, galactose, mannose, and fucose residues, which are also called ACAMP (apoptosis cell associated molecules), are essential for prompt recognition of apoptotic cells by phagocytes [Dini, 2000; Dini et al., 2002]. We recently reported [Chionna et al., 2003] that normal cells exposed to 6 mT static MF express on the cell surface significant amounts of galactose and mannose residues, which are responsible for their recognition by liver sinusoidal cells at a rate similar to that of liver sinusoidal cell recognition of apoptotic cells [Dini, 2004].

Moreover, Ca^{2+} ions as mediators of intracellular signaling are crucial for the development of apoptosis: an increase of $[Ca^{2+}]_i$ in cells committed to apoptosis, due to the emptying of intracellular $[Ca^{2+}]_i$ stores and to $[Ca^{2+}]_i$ influx from the extracellular medium, is a general phenomenon, independent of the apoptotic stimulus [Bian et al., 1997]. However, the role of

$[Ca^{2+}]_i$ increase during apoptosis is ambiguous because it exerts different effects in different cell systems [Magnelli et al., 1994; Teodori et al., 2002a,b]. Compounds inducing Ca^{2+} flux (such as thapsigargin or ionomycin) induce apoptosis in freshly explanted rat thymocytes; in contrast, the same induction of Ca^{2+} influx reduces the extent of stress-induced apoptosis in U937 cells and human lymphocytes, thus demonstrating an anti-apoptotic role of $[Ca^{2+}]_i$ [Fanelli et al., 1999; Teodori et al., 2002a,b; Chionna et al., 2003]. Therefore, an increase in $[Ca^{2+}]_i$ accompanies apoptosis both in cells where Ca^{2+} plays an anti-apoptotic role and in cells where Ca^{2+} prevents apoptosis [Teodori et al., 2002a,b]. Hep G2 cells seem to behave like thymocytes, which are not rescued from apoptosis by static MFs; indeed, apoptosis actually increased slightly in the presence of 6 mT static MF. The choice of cell system could explain in part the many conflicting results reported by different investigators who have failed to detect any apoptotic effects of MF [Teodori et al., 2002a,b].

Other possible effects of static MFs, such as an alteration of the gene pattern expression [Dini et al., manuscript submitted] and increased reactive oxygen species, which together with $[Ca^{2+}]_i$ influx modification could lead to perturbation of the apoptotic rate [Fanelli et al., 1999; Jajte, 2000; Chionna et al., 2003] cannot be excluded.

CONCLUSIONS

In the study of the interaction of static MFs with living organisms, many gaps in knowledge remain, requiring more research in order to reduce possible environmental health risks [Repacholi and Greenbaum, 1999] In this regard, it is important to consider the probable introduction of new technologies such as magnetically raised trains or the therapeutic use of MFs, for example, the exposure of patients to strong static MFs during magnetic resonance imaging (MRI) [Schenck, 2000]. Indeed, a fascinating new area that has been evolving in recent years is the coupling of MFs exposure with possible chemotherapy [Gray et al., 2000]. Therefore, it is essential to improve our knowledge of the biological effects (negative and positive) of MFs on living organisms. To date, acute or working environment exposure to static MFs at flux densities below 2 T have not been unequivocally found to have adverse health consequences. The data described in the present paper indicate that the biological effects of 6 mT static MF on Hep G2 cells are not cytotoxic. Further studies need to be carried out to ascertain whether, at longer exposure times than those investigated in the present study, the sub-lethal perturbations of the cells are permanent or reversible, and whether a point of no return exists during exposure to static MFs, after which the progressive accumulation of modifications could result in severe cellular damage leading to development of disease.

REFERENCES

Abbro L, Lanubile R, Dini L. 2004. Liver recognition of young and aged lymphocytes exposed to magnetic pollution. Recent Res Devel Cell Sci 1:83–97.

Albertini MC, Accorsi A, Citterio B, Burattini S, Piacentini MP, Uguccioni F, Piatti E. 2003. Morphological and biochemical modifications induced by a static magnetic field on *Fusarium culmorum*. Biochimie 85:963–970.

Bian X, Hughes FM, Jr., Huang Y, Cidlowski JA, Putney JW, Jr. 1997. Roles of cytoplasmic Ca^{2+} and intracellular Ca^{2+} stores in induction and suppression of apoptosis in S49 cells. Am J Physiol 272:C1241–C1249.

Bras W, Diakun GP, Maret G, Kramer H, Bordas J, Medrano FJ. 1998. The susceptibility of pure tubulin to high magnetic fields: A magnetic birefrengence and X-ray fiber diffration study. Biophysical J74:1509–1521.

Chionna A, Dwikat M, Panzarini E, Tenuzzo B, Carlà EC, Verri T, Pagliara P, Abbro L, Dini L. 2003. Cell shape and plasma membrane alterations after static magnetic fields exposure. Eur J Hystochem 47:299–308.

Cossarizza A, Monti D, Bersani F, Cantini M, Cadessi R, Sacchi A, Franceschi C. 1989. Extremely low frequency pulsed electromagnetic fields increase cell proliferation in lymphocytes from young and aged subjects. Biochem Biophys Res Commun 160:692–698.

Denegre JM, Valles JM, Jr., Lin K, Jordan WB. 1998. Cleavage planes in frog eggs altered by strong magnetic fields. Proc Natl Acad Sci USA 95:14729–14732.

Dini L. 2000. Clearance of apoptotic lymphocytes by human Kupffer cells. Phagocytosis of apoptotic cells in the liver: Role of lectin receptors and therapeutic advantages. In: Cameron RG, Feuer G, editors. Handbook of experimental pharmacology. Apoptosis and its modulation by drugs. Vol. 142. Heidelberg, Berlin: Springer-Verlag. pp 319–341.

Dini L, Pagliara P, Carlà EC. 2002. Phagocytosis of apoptotic cells by liver: A morphological study. Micron Res Techn 57:530–540.

Fadok VA, Chimini G. 2001. The phagocytosis of apoptotic cells. Semin Immunol 13:365–372.

Fanelli C, Coppola S, Barone R, Colussi C, Gualaldi G, Volpe P, Ghibelli L. 1999. Magnetic fields increase cell survival by inhibiting apoptosis via modulation of Ca^{++} influx. FASEB J 13:95–102.

Flipo D, Fournier M, Benquet C, Roux P, Le Boularie C, Pinsky C, La Bella FS, Krzystyniak K. 1998. Increased apoptosis, changes in intracellular Ca^{2+}, and functional alterations in lymphocytes and macrophages after in vitro exposure to static magnetic field. J Toxicol Environ Health 54:63–76.

Gartzke J, Lange K. 2002. Cellular target of weak magnetic fields: Ionic conduction along actin filaments of microvilli. Am J Physiol Cell Physiol 283:C1333–C1346.

Gobba F, Malagoli D, Ottaviani E. 2003. Effects of 50 Hz magnetic fields on fMLP-induced shape change in invertebrates immunocytes: The role of calcium ion channels. Bioelectronmagnetics 24:277–282.

Gray JR, Frith CH, Parker JD. 2000. In vivo enhancement of chemotherapy with static electric or magnetic fields. Bioelectronmagnetics 21:575–583.

Grynkiewicz G, Poenie M, Tsien RJ. 1995. A new generation of Ca^{2+} indicators with greatly improved fluorescence properties. J Biol Chem 260:3440–3450.

Hamada SH, Witkus R, Griffith R, Jr. 1989. Cell surface changes during electromagnetic field exposure. Exp Cell Biol 57: 1–10.

Hong FT. 1995. Magnetic field effects on biomolecules, cells, and living organisms. Biosystems 36:187–229.

Jajte JM. 2000. Programmed cell death as a biological function of electromagnetic fields at a frequency of (50/60 Hz). Med Pr 51:383–389.

Karasek M, Lerchl A. 2002. Melatonin and magnetic fields. Neuroendocrinol Lett 23:84–87.

Kheifets LI. 2001. Electric and magnetic field exposure and brain cancer: A review. Biolectromagnetics 5:S120–S131.

Lisi A, Pozzi D, Pasquali E, Rieti S, Girasole M, Cricenti A, Generosi R, Serafino AL, Congiu-Castellano A, Ravagnan G, Giuliani L, Grimaldi S. 2000. Three dimensional (3D) analysis of the morphological changes induced by 50 Hz magnetic field exposure on human lymphoblastoid cells (Raji). Bioelectromagnetics 21:46–51.

Magnelli L, Cinelli M, Turchetti A, Chiarugi VP. 1994. Bcl-2 overexpression abolishes early calcium waving preceding apoptosis in NIH-3T3 murine fibroblasts. Biochem Biophys Res Commun 204:84–90.

Ottaviani E, Malagoli D, Ferrari A, Tagliazucchi D, Conte A, Gobba F. 2002. 50 Hz magnetic fields of varying flux intensity affect cell shape changes ininvertebrate immunocytes: The role of potassium ion channels. Bioelectromagnetics 23: 292–297.

Paradisi S, Donelli G, Santini MS, Straface E, Malorni W. 1993. A 50 Hz magnetic field induces structural and biophysical changes in membranes. Bioelectronmagnetics 14:247–255.

Popov SV, Svitkina TM, Margolis LB, Tsong TY. 1991. Mechanism of cell protrusion formation in electrical field: The role of actin. Biochem Biophys Acta 1066:151–158.

Repacholi MH. 1998. Low-level exposure to radiofrequency electromagnetic fields: Health effects and research needs. Bioelectromagnetics 19:1–19.

Repacholi MH, Greenbaum B. 1999. Interaction of static and extremely low frequency electric and magnetic fields with living systems: Health effects and research needs. Bioelectronmagnetics 20:133–160.

Rieti S, Manni V, Lisi A, Giuliani L, Sacco D, D'Emilia E, Cricenti A, Generosi R, Luce M, Grimaldi S. 2004. SNOM and AFM microscopy techniques to study the effect of non-ionizing radiation on the morphological and biochemical properties of human keratinocytes cell line (HaCaT). J Microsc 213: 20–28.

Rosen AD. 1993. Membrane response to static magnetic fields: Effect of exposure duration. Biochem Biophys Acta 1148: 317–320.

Rosen AD. 2003. Mechanism of action of moderate-intensity static magnetic fields on biological systems. Cell Biochem Biophys 39:163–173.

Rosen MS, Rosen AD. 1990. Magnetic field influence on Paramecium motility. Life Sci 46:1509–1515.

Saffer JD, Phillips JL. 1996. Evaluating the biological aspescts of in vitro studies in bioelectromagnetics. Bioelectrochem Bioenerg 40:1–7.

Santoro N, Lisi A, Pozzi D, Pasquali E, Serafino A, Grimaldi S. 1997. Effect of extremely low frequency (ELF) magnetic field exposure on morphological and biophysical properties of human lymphoid cell line (Raji). Biochem Biophys Acta 1357:281–290.

Savill J, Fadok V. 2000. Corps clearance defines the meaning of cell death. Nature 407:784–787.

Schenck JF. 2000. Safety of strong, static magnetic fields. J Magn Reson Imaging 12:2–19.

Teodori L, Gohde W, Valente MG, Tagliaferri F, Coletti D, Perniconi B, Bergamaschi A, Cerella C, Ghibelli L. 2002a. Static magnetic fields affect calcium fluxes and inhibit stress-induced apoptosis in human glioblastoma cells. Cytometry 49:143–149.

Teodori L, Grabarek J, Smolewski P, Ghibelli L, Bergamaschi A, De Nicola M, Darzynkiewicz Z. 2002b. Exposure of cells to static magnetic fields accelerates loss of integrity of plasma membrane during apoptosis. Cytometry 49:113–118.

Walleczek J, Liburdy R. P. 1990. Nonthermal 60-Hz sinusoidal magnetic field exposure enhances $45Ca^{++}$ uptake in rat thymocytes: Dependence on mitogen activation. FEBS Lett 271:157.

Wartenberg D. 2001. Residential EMF exposure and childhood leukemia: Metanalysis and population attributable risk. Biolectromagnetics 5:S86–S104.